

UNCLASSIFIED

**Defense Technical Information Center
Compilation Part Notice**

ADP014325

TITLE: Nanoscale Analysis of a Co-SrTiO₃ Interface in a Magnetic Tunnel Junction

DISTRIBUTION: Approved for public release, distribution unlimited

This paper is part of the following report:

TITLE: Materials Research Society Symposium Proceedings. Volume 746. Magnetoelectronics and Magnetic Materials - Novel Phenomena and Advanced Characterization

To order the complete compilation report, use: ADA418228

The component part is provided here to allow users access to individually authored sections of proceedings, annals, symposia, etc. However, the component should be considered within the context of the overall compilation report and not as a stand-alone technical report.

The following component part numbers comprise the compilation report:

ADP014306 thru ADP014341

UNCLASSIFIED

Nanoscale analysis of a Co-SrTiO₃ interface in a Magnetic tunnel junction

J.-L. Maurice¹, F. Pailloux^{1*}, D. Imhoff², J.-P. Contour¹, A. Barthélémy¹, M. Bowen¹,
C. Colliex² and A. Fert¹

¹Unité Mixte de Physique CNRS/Thales, 91404 Orsay, France

²Laboratoire de Physique des Solides, Université Paris-Sud, 91405 Orsay, France

ABSTRACT

We use High Resolution Electron Microscopy together with Electron Energy Loss Spectroscopy to analyze the crystallography and the chemical configuration of a Co/SrTiO₃ interface in a Co/SrTiO₃/La_{2/3}Sr_{1/3}MnO₃ magnetic tunnel junction.

PACS: 75.47.-m, 75.70.Cn, 68.37.Lp, 79.20.Uv

INTRODUCTION

Magnetic tunnel barriers present a conduction that depends on the respective spin polarizations of the two electrodes. Because it is a half metal, the La_{2/3}Sr_{1/3}MnO₃ (LSMO) compound is very interesting as a probing electrode for spin-dependent spectroscopy: voltage-dependent measurements at low bias should in principle reflect the spin-dependent density of states of the other electrode. Several systems have thus been studied by varying the material of the second electrode (Co, FeNi) and also the nature of the insulator [SrTiO₃ (STO) amorphous Al₂O₃, Ce_{1-x}La_xO_{(2-x)/2}], as the insulator also plays a role as a spin filter [1], [2]. These studies outline the key role played by the interfaces in such devices. Our analytical work on the STO/LSMO interface is published elsewhere [3], [4], [5]. Here, we present the analysis of the Co/STO interface in a Co/STO/LSMO junction. This kind of junction still gives rise to TMR effects at 330K, which is quite close the T_c of the LSMO thin films used as first electrode. The understanding of the behavior of these heterostructures requires the use of characterization methods that can probe one monolayer at the interface. Transmission electron microscopy (TEM) in cross section is particularly suitable in such a case. In this paper, we present an atomic scale characterization by high resolution TEM (HRTEM) and electron energy loss spectroscopy (EELS) in scanning TEM (STEM).

More precisely in a Co/STO/LSMO tunnel junction, the atomic configuration at the Co/STO interface determines the polarization of the tunneling electrons that are emitted or accepted by the cobalt electrode. De Teresa *et al.* [1] have observed *inverse* magnetoresistance in Co/STO/LSMO tunnel junctions, suggesting that the spin of conduction electrons at the Co/STO interface is antiparallel to the magnetization. They explained that tunneling electrons through an STO barrier are d-band electrons and that the d-band in cobalt or at a cobalt surface [6] happens

*Now at Laboratoire de Métallurgie Physique, Université de Poitiers, 86962, Futurscope, France

to be larger at the Fermi level for *minority* spins. Recently, Oleinik *et al.* have performed electronic structure calculations of the fcc Co(100)/STO interface, considering various atomic configurations [7]. These authors concluded that the most stable interface configuration between fcc Co (100) and SrTiO₃ is Co/TiO₂, with Co atoms lying on top of O anions. With this configuration, they found a magnetic moment of $0.25\mu_B$ on the interfacial Ti cations. As this magnetic moment was aligned antiparallel to the magnetization of the Co layer, they claimed that this might be at the origin of the inverse-TMR observed by de Teresa *et al.*. Oleinik *et al.* also pointed out the lack of experimental structural data concerning such heterostructures. This is precisely what we bring here, on a junction prepared with the same equipment as that studied by De Teresa *et al.* [1].

GROWTH

We grow the oxide films by Pulsed Laser Deposition (PLD), a technique that allows the transfer of the cationic stoichiometry from the target to the substrate [8]. Using optimized growth parameters, thin LSMO films grown on (001) SrTiO₃ (STO) substrates exhibit physical properties more or less comparable to the bulk ones, depending on the deposited thickness [9]. In more detail, a frequency tripled Nd:YAG laser ($\lambda=355$ nm) has been focused on a sintered stoichiometric target of LSMO. During the deposition, the STO substrates have been heated to a temperature of 720°C and the oxygen pressure in the chamber has been set to 0.35 Torr. The STO 1.5-nm thin barrier was deposited in the conditions optima for LSMO (with the same oxygen pressure). At the end of the deposition, that pressure was raised to 300 Torr and maintained at this value during the cooling of the sample. The STO/LSMO interface is abrupt [4] and presents no significant chemical segregations [3].

Cobalt was deposited on top of STO by sputtering in another equipment. The transfer between the PLD and sputtering equipments has been performed under nitrogen, with a brief (< 1 min) exposition to ambient air.

EXPERIMENTAL METHODS

Cross-sectional samples for TEM have been thinned by mechanical polishing, using a tripod polisher to about 5 to 10 μm , then ion-milled using a Gatan-PIPS ion miller (Ar, 2.5keV, 6°) until electron transparent [10]. Transmission electron microscopy has been carried out using a Topcon EM002B electron microscope, operated at 200kV (0.19 nm spatial resolution). In order to interpret HRTEM images, we have compared the experimental pictures with simulated images calculated with the EMS software package using the multislice method [11]. We have determined the best imaging conditions by calculating thickness/defocus maps. Since Co is not oriented as to give a definite HRTEM contrast, we have optimized the STO/LSMO contrast. The best defocus values are between -30 nm and -40 nm for a sample thickness laying between 17.2 nm and 18.5 nm. Under these conditions, the bright dots observed in STO correspond to the projection of both atomic columns of strontium and TiO. The bright dots seen in the LSMO correspond to the projection of MnO atomic columns, whereas lanthanum/strontium columns are imaged weakly [3]. For the clarity of the interpretations, we refer to the pseudo-cubic unit cell of LSMO (instead of the R-3C rhombohedral one) for which the lattice parameter is $a_0 = 0.3873$ nm and the pseudo-cubic angle is $\alpha = 90.26^\circ$ [12]. This symmetry is preferred because of its similarity to the STO symmetry ($a_0 = 0.3905$ nm, $\alpha = 90^\circ$).

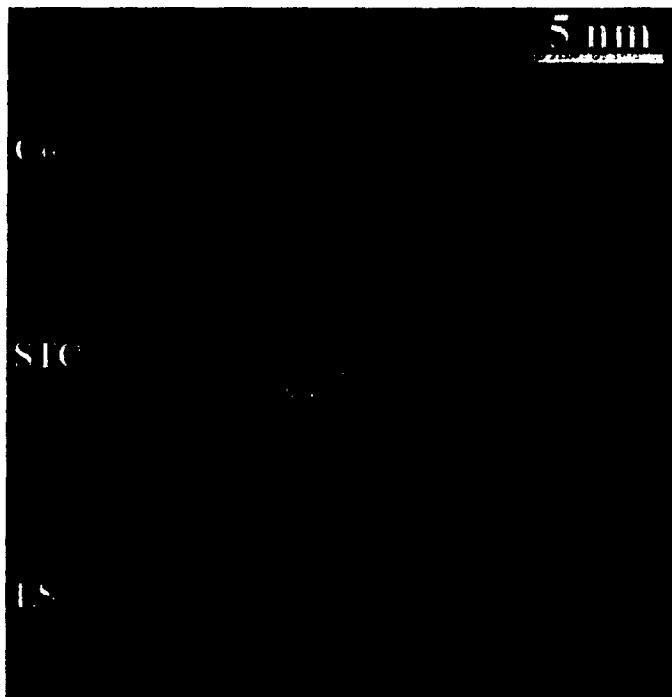


Figure 1. HRTEM picture of the Co/STO/LSMO tunnel junction. The white circles indicate the path and size of the probe used for the EELS spectrum lines.

EELS experiments have been performed in a VG HB 501 dedicated STEM, operated at 100 kV with a field emission gun and equipped with a Gatan-PEELS spectrometer coupled to a CCD detector by optical lenses. We have focused on the Energy-Loss Near Edge Structure (ELNES) of elements constituting the tunnel junction. Reference spectra for the studied edges (O-1s, Co-2p) have been recorded from the "bulk" part of the thin foil. Energy dispersions as low as 0.2eV have been used, leading to an energy resolution of about 0.6eV (measured on the zero-loss peak). The spectrum line method [13] has been employed to record several spectra across the interfaces. In this mode, the probe (0.7nm) is scanned across the interface along a line inclined of about 25° with respect to the interface (Fig. 1). The large amount of data recorded using this procedure have been processed using different mathematical tools including the Multivariate Statistical Analysis (MSA) technique and the Normalized Spatial Difference (NSD) [14], [15], the Non Negative Least Square (NNLS) fit to enhance particular features.

RESULTS AND DISCUSSION

In this section, we describe and discuss the atomic configuration at the Co/STO interface. Figure 2 is an overview of the whole Au/CoO/Co/STO/LSMO heterostructure deposited on a

(001) STO substrate. Electron diffraction patterns (not presented here) evidence that the Co layer is polycrystalline and textured. The digital diffractogram shown in inset of Fig. 2 corroborates that the growing planes of the cobalt layer are mainly the (001) planes of the hexagonal (hcp) structure of bulk Co. The main feature in this micrograph is the presence of steps at the Co/STO interface. Further examination of these steps reveals that their height is of the order of the lattice constant of STO (at equilibrium: 0.3905nm) and is the same for each step. These steps are periodically distributed along the interface, leading to a misorientation between the interface and the crystallographic planes of about 2°, which is roughly the nominal substrate misorientation. As stacking-faults (Ruddlesden-Popper faults) are observed in neither the LSMO nor the STO layer, and considering the height of the steps, we can state that the termination of the STO barrier is of the same type along the observed area of the sample. It means that the Co atoms located at the interface roughly have the same environment whatever their location.

A thorough investigation of HRTEM contrast using image simulation allows us to discriminate the various cationic sites in both the LSMO and STO layers. The comparison between experimental and simulated through-focus series [3] leads to the conclusion that, in Fig. 1 and Fig. 2, the large bright dots in the LSMO layer correspond to the Mn site, whereas the small bright dots are the image of the $\text{La}_{2/3}\text{Sr}_{1/3}$ atomic columns. The situation is a little more complex in the case of STO: the bright dots for both cationic site (Sr and Ti) give roughly the same intensity in experimental pictures. As we have shown previously [3], the perovskite stacking sequence is kept across the LSMO/STO interface. It is thus possible to discriminate between the Sr and Ti site in the STO layer: Ti cations are located in the continuation of the Mn atomic rows. The next step in the investigation is the determination of the atomic plane of the STO layer on which the Co layer will be deposited. HRTEM images reveal that on the terraces between the steps described above, the last well-crystallized layer is mainly a TiO_2 layer (Fig. 1),

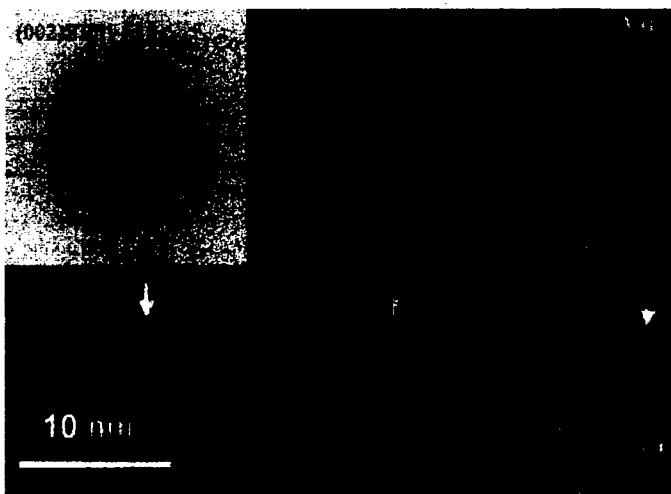


Figure 2. The whole stack of layers, from top to bottom: Au/CoO/Co/STO/LSMO (STO substrate not shown).

which is consistent with a recent work indicating that the last ordered layer at an STO {100} surface annealed under O₂ at high temperature is made of TiO₆ octahedra [16]. Between that layer and the first Co metallic layers, the transition plane exhibits in Fig. 2 weaker white dots at the places of the Sr columns of STO, and a contrast increase for the two first planes of Co. However, these details do not show in Fig. 1, which is taken at a different defocus.

Further information about this layer is obtained by EELS. Using signal processing routines such as MSA and NSD, we have observed that the O-1s edge is the combination of two signals at the STO/Co interface: the spectra acquired as the probe is located at the interface are a combination of those coming from STO and cobalt monoxide (CoO) (Fig. 3). Moreover, the non-negative least square (NNLS) fit of the whole spectrum line with the internal STO and CoO references confirms the presence of CoO-type bonding over a width of the order of a nanometer at the interface (Fig. 3b). The Co-2p edge also experiences a change of its shape at the Co/STO interface, which corroborates the previous analysis. This tends to indicate that the experimental Co/STO interface is not as simple as the one assumed in the calculation [7], as it includes an intermediate layer. Whether that layer acts as a supplement to the barrier or not, and whether it is paramagnetic or carries a magnetization opposite to that of cobalt (Néel temperature of bulk antiferromagnetic CoO is 292K [17]), remains to be demonstrated.

CONCLUSIONS

We have analyzed an interface that had been the object of magneto-transport measurements [1] and electronic structure calculations [7]. The latter was based on the assumption of fcc cobalt,

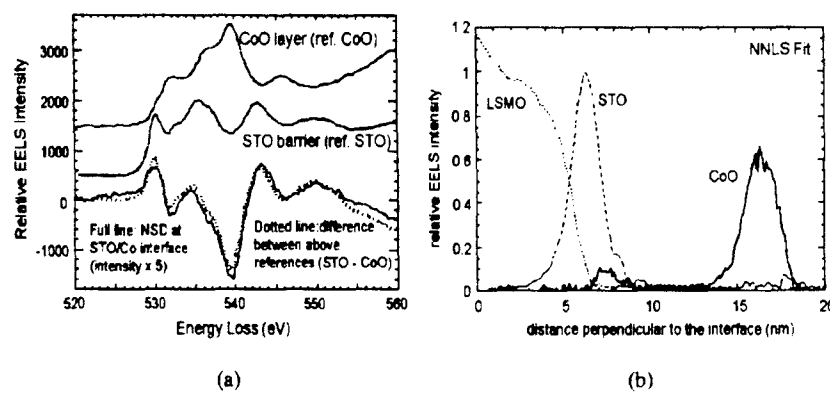


Figure 3. (a) EELS O-1s edges recorded in the CoO and STO layers (top) to serve as references for the analysis of the same edge at the Co/STO interface. Bottom: normalized spatial difference (NSD) spectrum at the interface (full line) compared with a weighted difference between CoO and STO references (dotted line). (b) Non-negative least square (NNLS) fit of the O-1s edge spectrum line, using the O-1s edges in the LSMO, STO and CoO layers as internal references, which unambiguously indicates the presence of CoO at the interface over a distance of the order of the nm.

(100) oriented. The first fact we bring is that the actual layer is hcp and polycrystalline, with a 0001 texture. The calculations [7] involving energy minimization are structure specific and cannot therefore apply to our particular experimental device. However, the interpretations of the inverse magnetoresistance in terms of cobalt density of state [1] can still hold as the d-band configuration at the Fermi level does not significantly depend on whether the cobalt is fcc or hcp or on its orientation. On the other hand, the layer of atomic thickness seen at the interface (be it CoO or other) probably influences the TMR but how this influence is important is difficult to assess.

ACKNOWLEDGEMENTS

We thank Prof. Revcolevschi (Université Paris-Sud) for providing the LSMO target, M. Bibès, F. Petroff (UMP CNRS/Thales), T. Sikora (LPS Université Paris-Sud) for fruitful discussions, and Mr Jacquet (UMP CNRS/Thales) for his help with PLD.

REFERENCES

- [1] J-M De Teresa, A. Barthélémy, A. Fert, J-P. Contour, R. Lyonnet, F. Montaigne, P. Seneor, A. Vaures, *Phys. Rev. Lett.* **82**, 4288 (1999); *Science* **286**, 507. (1999)
- [2] A. Fert *et al.*, *Materials. Science and. Engineering* **B84**, 1 (2001).
- [3] F. Pailloux, D. Imhoff, T. Sikora, A. Barthélémy, J.-L. Maurice, J.-P. Contour, C. Colliex, A. Fert, *Phys. Rev.* **B66**, 014417 (2002).
- [4] J.-L. Maurice, R. Lyonnet, J.P. Contour, *J. Magn. Magn. Mater.* **211**, 91 (2000).
- [5] L. Samet, D. Imhoff, J.-L. Maurice, J.-P. Contour, A. Gloter, T. Manoubi, A. Fert, C. Colliex, *to be published*
- [6] K. Wang, PhD thesis, New York University, 1999.
- [7] I.I. Oleinik, E.Y. Tsymbal, D.G. Pettaffor, *Phys. Rev. B* **65**, 020401(R) (2002).
- [8] J.P. Contour, C. Sant, D. Ravelosona, B. Fischer, L. Patlagan, *Jpn. J. Appl. Phys.* **32**, 1134 (1993).
- [9] J.-L. Maurice, F. Pailloux, A. Barthélémy, A. Rocher, O. Durand, R. Lyonnet, J.-P. Contour, *Appl. Surf. Sci.* **188**, 176 (2002).
- [10] J. Benedict, R. Anderson, S. Klepeis, M. Chaker, Mater. Res. Soc. Symp. Proc. 199 (1990) 189.
- [11] P. Stadelman, *Ultramicroscopy* **21**, 131 (1987).
- [12] A. Hammouche, E. Siebert, A. Hammou, *Mat. Res. Bull.* **24**, 367 (1989).
- [13] C. Jeanguillaume and C. Colliex, *Ultramicroscopy* **28**, 252 (1989).
- [14] N. Bonnet, N. Brun and C. Colliex, *Ultramicroscopy* **77**, 97 (1999).
- [15] P. Trebbia and N. Bonnet, *Ultramicroscopy* **34**, 165 (1990).
- [16] N. Erdman, K. R. Poepelmeier, M. Asta, O. Warschkow, D. E. Ellis and L. D. Marks, *Nature* **419**, 55 (2002).
- [17] See, e.g.: P.A. Cox, *Transition Metal Oxides* (Clarendon Press, Oxford, 1995).